A Comparison of Hole-filling Methods for 3D Medical Data Reconstruction and Visualization

Chan Vei Siang & Farhan Mohamed
School of Computing
Faculty of Engineering
Universiti Teknologi Malaysia
81310 UTM Johor Bahru, Johor, Malaysia
Email: chanveisiang@hotmail.my

Abstract—**3D medical imaging can help the physicians to understand the patient anatomy, such as 3D ultrasound and 3D CT scan. In the case of 3D ultrasound reconstruction, the pixel nearest neighbour is one of the popular methods used. The hole-filling method in pixel nearest neighbour can fill in the empty voxel data which is not captured by the ultrasound. Thus, this paper studied the various hole-filling methods in the pixel nearest neighbour method to reconstruct the missing voxels. Besides that, an alternative method is also introduced based on the modified butterfly interpolation scheme. The experiment setup is designed to test the efficiency of the hole-filling method for 3D medical data visualisation by using mean absolute error as well as qualitatively compare the visualization of the reconstruction results. The proposed method can extract smooth skin from the reconstruction volume, although it has a high average MAE result.**

Keywords—**Medical imaging, 3D reconstruction, scientific visualization, ultrasound, CT data set, pixel nearest neighbor, hole-filling method**

I. INTRODUCTION

The medical imaging is essential to the physicians in diagnosis and analysis by visualising the inner anatomy of the patient. The medical imaging modalities are such as magnetic resonance imaging (MRI), ultrasound imaging and computer tomography (CT) imaging. Conventionally, the physicians are still using 2D medical images for diagnosis and decision making. However, the 2D medical image is painful to interpret, especially by the beginner and required much practise to master by mentally construct the 2D images into 3D volume. For example, in the ultrasound imaging, the 2D imaging in

ultrasound possessed the limitations [1] such as time-consuming for decision making, difficult to measure organ volume and the anatomy feature obscures some views. Hence, 3D medical data reconstruction can improve and solve the limitation of 2D medical imaging.

The 3D medical data reconstruction in ultrasound has gained attention among the practitioners and researchers alike since the 90s. The 3D ultrasound reconstruction generates a 3D volume from a series of 2D ultrasound images by using the volume reconstruction method [2]. The volume reconstruction method is the interpolation and approximation algorithm to reconstruct the volume. There are various volume reconstruction methods have been researched, and the pixel nearest neighbour (PNN) is still favourable among the researchers due to its simplicity, and it does not require much of the computational power. Besides that, many improvements have been proposed to create optimal reconstruction results [3–5].

The PNN has two important steps, which are bin-filling step and hole-filling step [3]. First, the bin-filling step is used to fill the voxels in a 3D volume grid based on each pixel of the acquired 2D ultrasound images. Next, the hole-filling method is used to calculate and fill the empty voxel found in the bin-filled 3D volume grid, to reconstruct the missing voxels based on its nearby voxel values. However, the main problem found in the PNN from previous works [4], [6], shows that most traditional hole-filling methods tend to blur the reconstruction result. There are also some artefacts have been observed on the boundaries between the bin-filled and the hole-filled regions.

In this paper, we focused on the hole-filling methods in the

PNN to fill the missing volume information in a standard data set, which will be the basis for future studies in the 3D ultrasound reconstruction. An alternative hole-filling method is also proposed based on the modified butterfly interpolation scheme.

The arrangement of this paper is as follows. Section II explains the materials and methods used in this experiment. The result and evaluation are presented in Section III. Then, Section IV discusses the results. The paper is closed by the conclusion and future work in Section V.

II. MATERIALS AND METHODS

A. Data set

This research project used the *headsq* CT scan data set as the test's subject to compare the various hole-filling methods. The CT data set is provided by Virtualization Toolkit (VTK) [7]. A CT image consists of different grey levels that represent different inner anatomy features, such as black colour normally represents air or nasal passage, grey colour for soft tissues, and white colour for bone. Fig. 1 shows an example of CT image of a cross-sectional head from the *headsq* CT data set. This data set contains a total of 93 slices with 1.5 mm spacing between the slices, and each slice has 256×256 pixels with 0.8 mm spacing between the pixels. The grey level of each pixel is in 12 bits. Hence, each pixel takes up two 8-bits memory spaces and are in little-endian arrangement. Fig. 2 shows the skin extracted from the *headsq* CT data set.

The reason for the use of CT data set is that it has the complete data with a minimum number of holes, as the data are taken millimetre by millimetre. Therefore, it can be reconstructed into a high dimension of 3D volume. This feature is very important for the qualitative analysis to test the accuracy of the various hole-filling method. It is also widely available to download from the VTK's source.
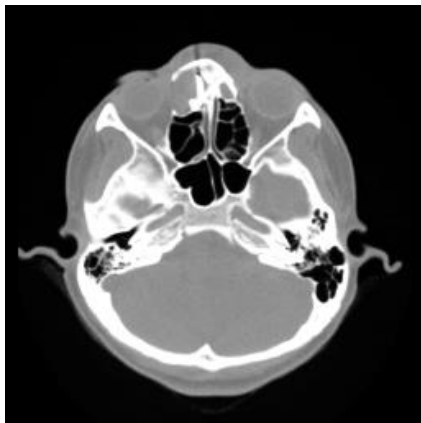

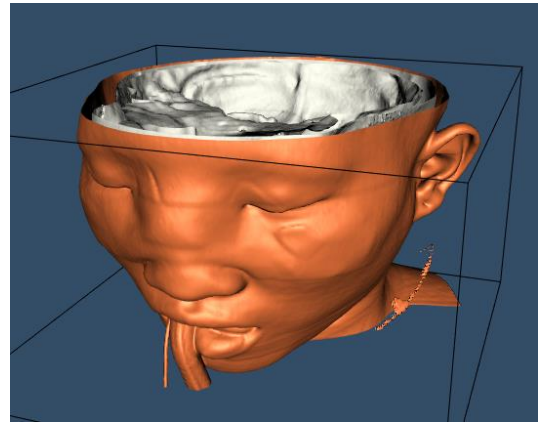Fig. 1. Example of a CT image that shows cross-sectional head

Fig. 2. The skin extracted from the CT scan data set [7]

B. Hole-filling Methods

The hole-filling method uses interpolation techniques to estimate the value of the empty voxel or hole based on the nearby filled voxel values. This research study uses the hole-filling methods, which include mean operation, median operation, Olympic operation and oriented sticks method. A proposed method using the modified butterfly interpolation scheme is also conducted. The hole-filling methods are discussed in detail as follows:

1) Mean Operation

The mean operation calculates the averaged sum of nearby filled voxels around the empty voxel and assigns the resultant value into that empty voxel. The nearby filled voxels are chosen if each voxel is within a kernel of the specified distance around the empty voxel. Fig. 3 shows the 26 neighbour voxels around the empty voxel with a distance of r = 1.
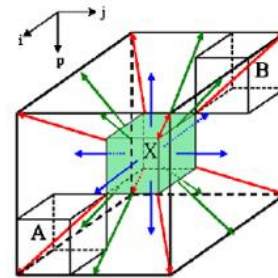

Fig. 3. The 26 neighbour voxels [6]

2) Median Operation

The median operation arranges the nearby filled voxels in ascending order and get the middle value to fill the hole. The median operation uses a kernel size of *r* = 1, as shown in Fig. 3.

3) Olympic Operation

In the Olympic operation, the 26 nearby filled voxels are also arranged in order as that in the median operation. Then, the removal of n% of the upper and lower values are performed to remove the outlier voxel values. Lastly, the remaining voxel values are averaged to fill the empty voxel. The Olympic operation also uses a kernel size of $r = 1$, as shown in Fig. 3.

4) Oriented Sticks Hole-filling Method

The oriented sticks hole-filling method uses a stick to search for the nearby filled voxels [5]. A stick is represented as a pair of opposite direction voxels. In this case, a maximum of 13 sticks is used, as shown in Fig. 4. There are two stages involved in this method. The first stage is to search for the sticks around the hole. The stick is obtained when two filled voxels along with the stick are found [5]. Then, the stick intensity is calculated based on the linear interpolation between the filled voxels. On the other hand, the stick is ignored if two filled voxels are not found along with the sticks after reaching a specified maximum length [5]. We set the maximum length to 3. In the next stage, the stick intensities with minimum length are chosen from the sticks collected in the first stage, to fill the hole by performing the distance weighted average as shown as follows:

$$hole = \frac{\sum_{i=1}^{N}(intensity_i/length_i)}{\sum_{i=1}^{N}(1/length_i)} \quad (1)$$

where N is the total number of sticks, $intensity_i$ is the intensity of stick i, and $length_i$ is the length of stick i.
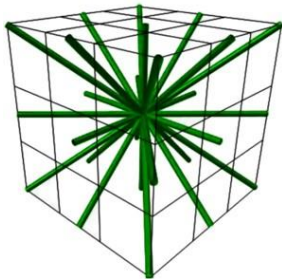

Fig. 4. The 13 sticks around the empty voxel [5]

5) Modified Butterfly Interpolation Scheme

This method employed the modified butterfly interpolation scheme, which is explained in detail in Subsection C.

C. Modified Butterfly Interpolation Scheme

Normally, the butterfly interpolation scheme is used in the subdivision of the surface to create a smooth surface by creating a new vertex on edge [8], [9]. Due to this characteristic, the use of a butterfly stencil map to fill the new value into the hole is proposed. As shown in Fig. 5, there are two types of butterfly stencil map where:

(a) the voxels $A1$ and $A2$ along the butterfly edge are both of valence, $K = 6$;

(b) there is at least one neighbour voxel along the butterfly edge has K not equal to 6, which is known as the extraordinary voxel (q).
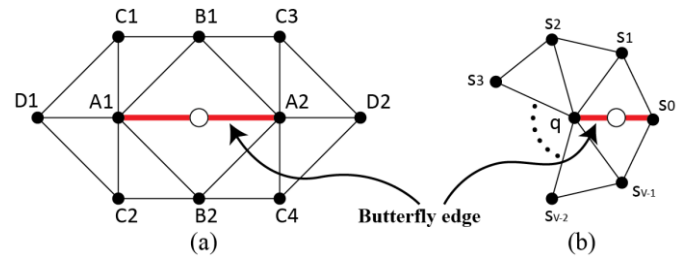

Fig. 5. The butterfly stencil: (a) 10-points stencil; (b) stencil with an extraordinary voxel. The white point is the empty voxel to be filled. The bold red line represents the butterfly edge.
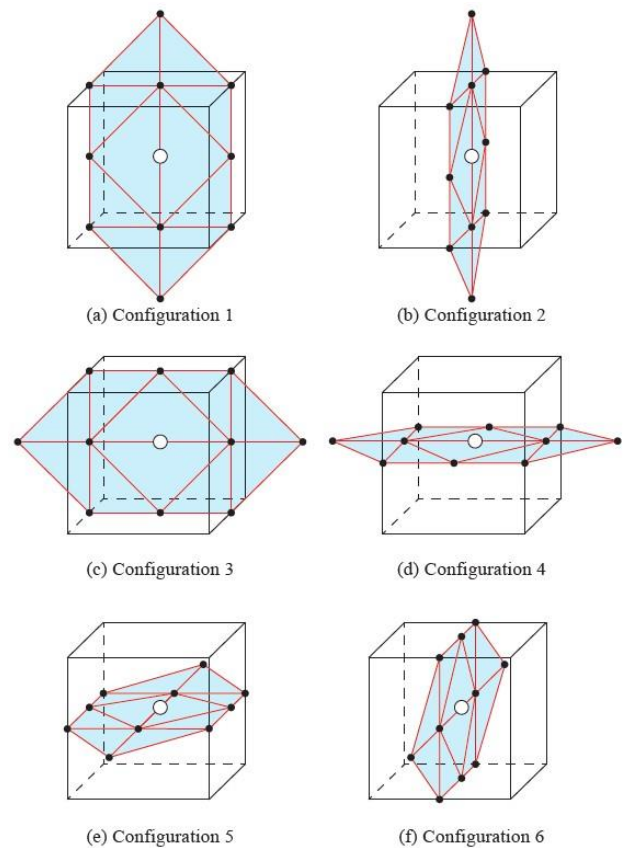

Fig. 6. The six butterfly configurations

We have designed this method in two stages. The first stage is to determine which butterfly stencil map or voxels network to use. Fig. 6 shows the six butterfly configurations. Similar to the oriented sticks method, the butterfly edge traverses along the direction in search for filled voxels $A1$ and $A2$. The butterfly map is found if the edge found both voxels within the specified range. We set the upper range to 3. A total of 6 edge directions are searched. The selection is based on the butterfly configuration

with the most number of voxels (a combination of voxels *A, B, C, D*).

In the second stage, the butterfly intensities of each selected configuration are calculated based on the following cases:

(a) **The butterfly edge connects two voxels of *K* = 6:** Equation (2) is used to calculate the butterfly intensity. The parameter *w* is set to 0.

(b) **The butterfly edge connects an extraordinary voxel and a voxel with *K* = 6:** There are three types of calculation based on the valence *K* of an extraordinary voxel. If *K* = 3, Equation (3) is used. Equation (4) is used if *K* = 4 and Equation (5) is selected if *K* = 5.

(c) **The butterfly edge connects two extraordinary voxels:** Both the extraordinary voxels perform the calculation based on case (b) and are averaged to get the final butterfly intensity.

$$a = \frac{1}{2} - w; b = \frac{1}{8} + 2w; c = -\frac{1}{16} - w; d = w \quad (2)$$

$$K = 3; q = \frac{3}{4}; s_0 = \frac{5}{12}; s_{1,2} = -\frac{1}{2} \quad (3)$$

$$K = 4; q = \frac{3}{4}; s_0 = \frac{3}{8}; s_{1,3} = 0; s_2 = -\frac{1}{8} \quad (4)$$

$$K = 5; q = \frac{3}{4};$$
$$s_j = \left(\frac{1}{4} + \cos\left(\frac{2\pi j}{K}\right) + \frac{1}{2}\cos\left(\frac{4\pi j}{K}\right)\right)/K \quad (5)$$

If there is more than one butterfly intensity, the butterfly intensities are averaged to fill the empty voxel.

D. Experiment Setup

The experiment is setup to test the efficiency of the existing hole-filling methods and the proposed method. Firstly, the CT data set is bin-filled into the volume. In order to mimic the holes and gaps as found in the ultrasound data, the artificial holes are created in the bin-filled volume. The hole removal percentages used is 300%, which is the removal of slice *n – 1* to slice *n + 1* slice in the axial direction. The value *n* is the selected CT data slices which are 7, 14, 21 and 28. Each *n* and its *n ± 1* slices are grouped as a large gap of holes and thus, there are four group of holes. Fig. 9 (b) shows the skin extracted from the 300% removal of CT scan data slices. In the hole-filling step, the methods presented in Subsection B are used for the 3D reconstruction.

In order to evaluate the efficiency and accuracy of hole-filling methods, there are two comparative studies have been done: (1) the qualitative analysis based on the comparison between 2D reconstructed slices and original slice, as well as the comparison of skin extraction between the original data set and reconstructed data set; and (2) the quantitative analysis calculates the mean absolute error (MAE) to evaluate the interpolation error in the reconstruction results between an original slice and 2D reconstructed slices [10]. The MAE is formulated as follow:

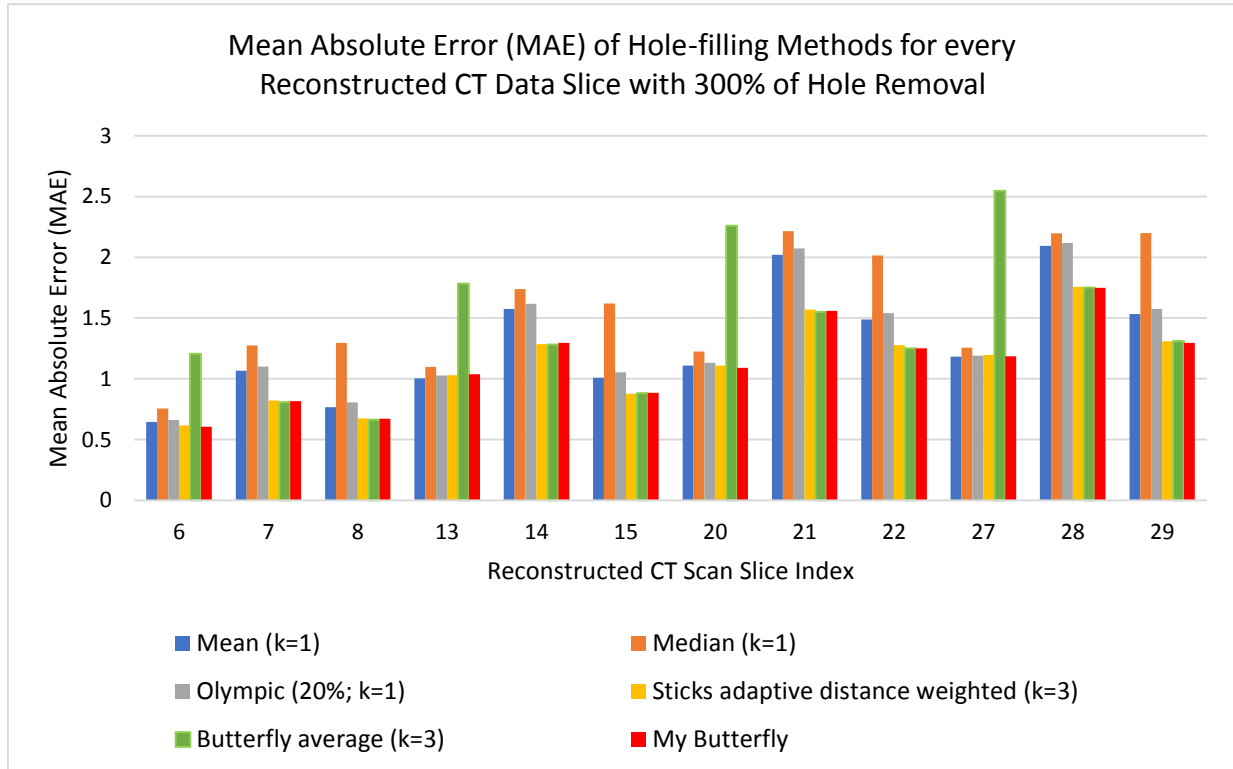$$MAE = \frac{1}{N}\sum_{i=1}^{N}|p_i - q_i| \quad (6)$$

Fig. 7. The MAE of hole-filling methods for every reconstructed CT scan slice with 300% hole removal

The *N* is the total number of pixels in the image slice. The p_i represents the pixel in the original slice and q_i represents the pixel in the reconstructed slice. The lower the MAE, the lower the interpolation error and the higher the accuracy of the hole-filling method.

The 3D visualisation method is also implemented to visualise the 3D CT data set by using the VTK. The marching cubes algorithm is used to extract the skin or surface data from the CT data set and reconstructed data set. Therefore, the comparison of the skin extraction between the original CT data set and reconstructed results can be performed.

III. RESULTS AND EVALUATION

A. Quantitative Analysis

The comparison between various hole-filling method is conducted using the mean absolute error (MAE) to determine the total interpolation error [11] in the reconstruction results. Fig 7 shows the MAE of hole-filling methods for every reconstructed CT data slice with 300% hole removal. Table I shows the average and standard deviation of MAE for this experiment.

Among the hole-filling methods, the result shows that the oriented sticks method is the most efficient hole-filling method with the lowest averaged MAE value, which is 1.12683. It is followed by the mean operation and Olympic operation, with the average MAE of 1.29074 and 1.32464, respectively. The observation also shows that most of the hole-filling methods have the highest reconstruction error when on the *n* slice in every group of holes (7, 14, 21, 28), as shown in Fig. 7, except the modified butterfly interpolation method. Besides that, we can observe that the modified butterfly interpolation method in each group of holes has the highest MAE in the *n – 1* slice, but the interpolation error decreased when it reconstructed through *n* and *n + 1* slices. The MAE values on *n* and *n + 1* slices of modified butterfly interpolation method are closed to that of the oriented sticks method.

TABLE I. The average and standard deviation of MAE for every reconstructed CT data slice with 300% hole removal

Hole-filling Methods	Average	Standard Deviation
Mean	1.29074	0.43798
Median	1.57428	0.47378
Olympic	1.32464	0.44321
Oriented Sticks	1.12683	0.33031
Modified Butterfly	1.44163	0.54467

(a) Original *headsq14*.

(b) *headsq14* after mean operation.

(c) *headsq14* after median operation.

(d) *headsq14* after Olympic operation.

(e) *headsq14* after oriented sticks method.
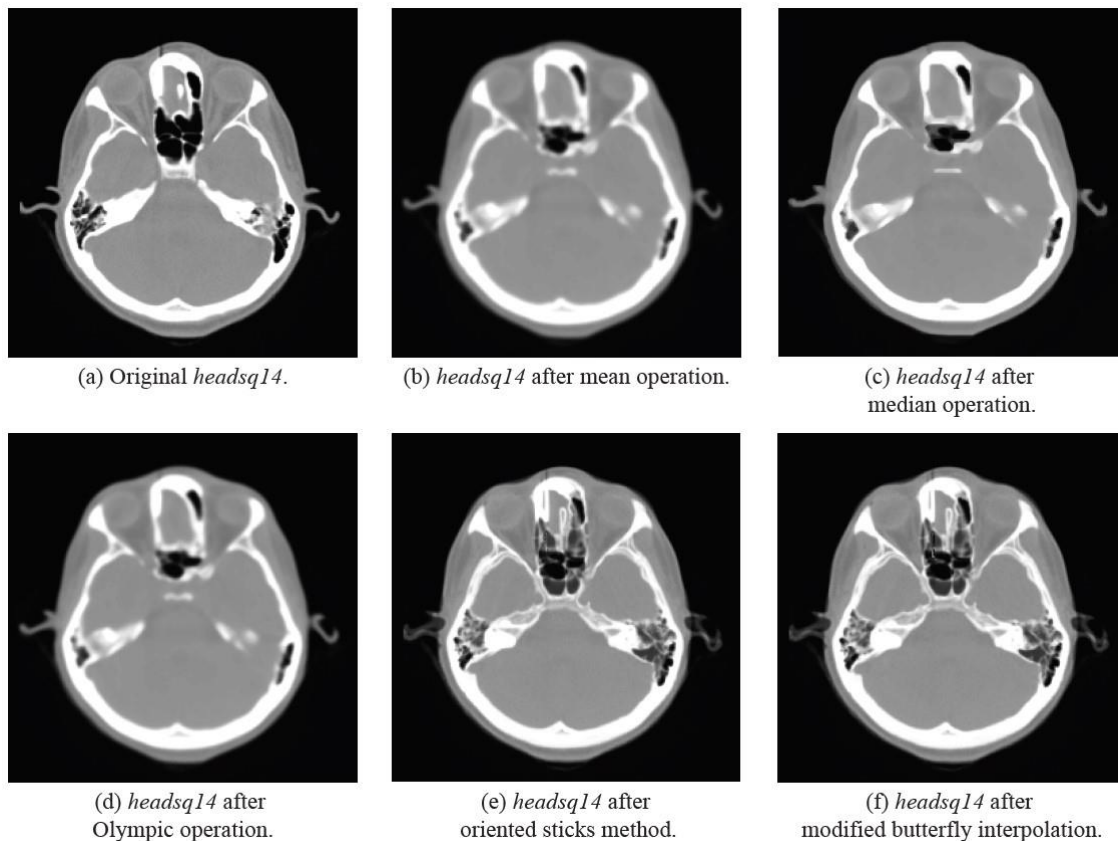
(f) *headsq14* after modified butterfly interpolation.

Fig. 8. The comparison between the original slice and the 2D reconstructed slices of *headsq14* in the 300% hole removal experiment

(a) Original *headsq*.

(b) Original *headsq* with artificial hole.

(c) *headsq* after mean operation.

(d) *headsq* after median operation.

(e) *headsq* after Olympic operation.

(f) *headsq* after oriented sticks method.
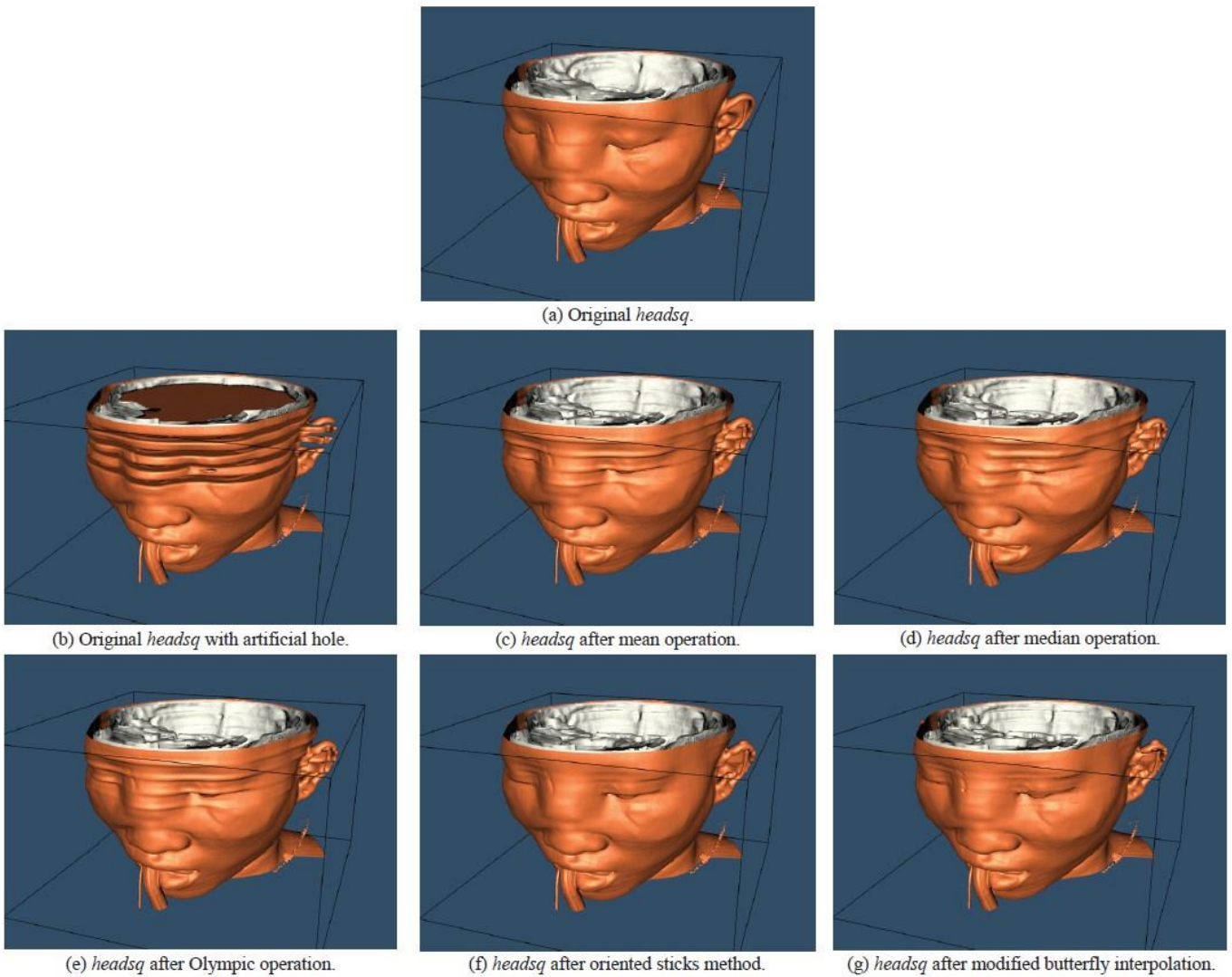
(g) *headsq* after modified butterfly interpolation.

Fig. 9. The comparison between skin extraction of reconstructed CT data for every hole-filling method with 300% hole removal

B. Qualitative Analysis

The CT scan of slice 14, also known as *headsq14,* is used for the first qualitative analysis. The image data is taken from the cross-sectional region across the eyelid on the head and is perpendicular to the spine. The eyes and bridge of the nose can be observed on the top region of the head and the ears are on the side of the head. Fig. 8 shows the comparison between the 2D reconstructed slices and the original slice of *headsq14* in the 300% hole removal experiment. It is observed that the use of oriented sticks method and modified butterfly interpolation can preserve relatively sharper features of the bone in comparison to other hole-filling methods. Most of the bone features are lost during the hole-filling step for mean, median and Olympic operation. However, both oriented sticks method and modified butterfly method have shown some reconstruction error at the ears when compared to the original slice.

The second qualitative analysis is to compare the 3D surface or skin extraction between the original data set and reconstructed data set using various hole-filling methods, as shown in Fig. 9. The 300% hole removal is employed four times in the original data set, as shown in Fig 9 (b). Again, the oriented sticks method and modified butterfly method show smooth skin extraction around the hole removal region, which is the eyelids and bridge of the nose. Consistent with the first qualitative analysis, both methods have experienced some reconstruction error around the ears. On the contrary, the facial features around the hole removal region do not preserve accurately for the mean, median and Olympic operation. However, the median operation shows smooth surface rendering around the bridge of the nose.

IV. DISCUSSION

Among the various hole-filling methods, the oriented sticks method has the lowest reconstruction error when compared to the original data set, due to its lowest MAE result. Therefore, it is the most accurate hole-filling methods, and it also showed that the linear interpolation is working better than averaging the nearby voxels, such as in mean operation and Olympic operation.

Our proposed modified butterfly interpolation method does not perform well on the $n – 1$ slice in every group of holes, but its reconstruction error decreases when reconstructed through n and $n + 1$ slices, because of the increase of butterfly edge $A1 – A2$ in both direction when searching for the suitable butterfly configurations. Since on the $n – 1$ slice, the edge needs to traverse a minimum distance of 3 in both directions to get the filled voxels for vertices $A1$ and $A2$ which caused the hole-filled value to deviate greatly from the original value. The qualitative analysis result also showed that the modified butterfly interpolation scheme could provide a smooth skin extraction that is relatively identical to the original skin surface, although its MAE is higher than the mean operation. This result is due to the characteristic of the modified butterfly method to subdivide the surface.

The main limitation in the current research study is the use of CT scan data set instead of the real ultrasound data set. The current research progress is to create the artificial holes in the CT scan data set to mimic the holes as found in the process of 3D ultrasound reconstruction and then the hole-filling methods are used to reconstruct the missing voxels information. Therefore, this case study does not consider the noises and artefacts that are found in the ultrasound images. The hole-filling methods found in this research study will be the basis for future studies in the 3D ultrasound reconstruction.

V. CONCLUSION AND FUTURE WORK

The 3D medical imaging can improve the work of physician as it can provide better visualisation for analysis and diagnosis purpose. In this paper, various hole-filling methods in the PNN to fill the holes in a standard data set are studied. An alternative hole-filling method is also proposed based on the modified butterfly interpolation scheme. The efficiency of the hole-filling methods is also tested by using MAE, as well as by analysed the reconstructed images and skin extraction of the reconstructed data set. For the future work, the modified butterfly interpolation method needs to improve in term of the increase of butterfly configuration to cover possible butterfly stencil map. Besides that, the adaptive weighted distance can also be applied to fill in the empty voxel which is inspired by the oriented sticks method.

REFERENCES

[1] Fenster, A., Downey, D. B., & Cardinal, H. N. (2001). Three-dimensional Ultrasound Imaging. *Physics in Medicine and Biology*, 46(5), R67. https://doi.org/10.1088/0031-9155/46/5/201.

[2] Siang, C. V., Mohamed, F., Mat Isham, M. I., Azimi Yusoff, Y., Abd Aziz, A. A., & Ekashanti Octorina Dewi, D. (2019). A Framework of Position Tracked Freehand 3D Ultrasound Reconstruction Using Game Controller and Pixel Nearest Neighbour Method for Marching Cubes Volume Visualization. *2018 IEEE Conference on Big Data and Analytics, ICBDA 2018*. https://doi.org/10.1109/ICBDAA.2018.8629650.

[3] Purnama, K. E., Wilkinson, M. H. F., Veldhuizen, A. G., Van Ooijen, P. M. A., Lubbers, J., Burgerhof, J. G. M., … Verkerke, G. J. (2010). A Framework for Human Spine Imaging Using a Freehand 3D Ultrasound System. *Technology and Health Care*, 18(1), 1-17. https://doi.org/10.3233/THC-2010-0565.

[4] Wen, T., Zhu, Q., Qin, W., Li, L., Yang, F., Xie, Y., & Gu, J. (2013). An Accurate and Effective FMM-based Approach for Freehand 3D Ultrasound Reconstruction. *Biomedical Signal Processing and Control*, 8(6), 645-656. https://doi.org/10.1016/j.bspc.2013.05.009.

[5] Vaughan, T., Lasso, A., Ungi, T., & Fichtinger, G. (2015). Hole Filling with Oriented Sticks in Ultrasound Volume Reconstruction Volume Reconstruction. *Journal of Medical Imaging*, 2(3). https://doi.org/10.1117/1.JMI.2.3.034002.

[6] Dewi, D. E. O., Wilkinson, M. H. F., Mengko, T. L. R., Purnama, I. K. E., Van Ooijen, P. M. A., Veldhuizen, A. G., … Verkerke, G. J. (2009). 3D Ultrasound Reconstruction of Spinal Images Using an Improved Olympic Hole-filling Method. *International Conference on Instrumentation, Communication, Information Technology, and Biomedical Engineering 2009, ICICI-BME 2009New York: IEEE (The Institute of Electrical and Electronics Engineers)*, (pp. 350-354). https://doi.org/10.1109/ICICI-BME.2009.5417235.

[7] W. J. Schroeder, B. Lorensen, & K. Martin. (2004). *The Visualization Toolkit: An Object-oriented Approach to 3D Graphics*. Kitware.

[8] Dyn, N., Levine, D., & Gregory, J. A. (1990). A Butterfly Subdivision Scheme for Surface Interpolation with Tension Control. *ACM Transactions on Graphics*, 9(2), 160-169. https://doi.org/10.1145/78956.78958.

[9] Zorin, D., Schröder, P., & Sweldens, W. (1996). Interpolating Subdivision for Meshes with Arbitrary Topology, 189-192.

[10] Dewi, D. E. O., Mengko, T. L. R., Purnama, I. K. E., Veldhuizen, A. G., & Wilkinson, M. H. F. (2010). An Improved Olympic Hole-Filling Method for Ultrasound Volume Reconstruction of Human Spine. *International Journal of E-Health and Medical Communications*, 1(3), 28-40.

[11] Willmott, C. J., & Matsuura, K. (2005). Advantages of The Mean Absolute Error (MAE) over the Root Mean Square Error (RMSE). *Climate Research*, 30(1), 79-82. Retrieved from http://climate.geog.udel.edu/~climate/publication_html/Pdf/WM_CR_05.pdf.